We are IntechOpen, the world's leading publisher of Open Access books Built by scientists, for scientists

6,900
Open access books available

185,000
International authors and editors

200M
Downloads

Our authors are among the

154
Countries delivered to

TOP 1%
most cited scientists

12.2%
Contributors from top 500 universities

WEB OF SCIENCE™

Selection of our books indexed in the Book Citation Index in Web of Science™ Core Collection (BKCI)

Interested in publishing with us?
Contact book.department@intechopen.com

Numbers displayed above are based on latest data collected.
For more information visit www.intechopen.com

Chapter 5

The Role of Sulfur-Related Species in Oxygen Reduction Reactions

Dan Xu and Winston Duo Wu

Additional information is available at the end of the chapter

http://dx.doi.org/10.5772/intechopen.78647

Abstract

Heteroatom (metal and nonmetal) doping is essential to achieve excellent oxygen reduction reaction (ORR) activity of carbon materials. Among the heteroatoms that have been studied to date, sulfur (S) doping, including metal sulfides and sulfur atoms, has attracted tremendous attention. Since S-doping can modify spin density distributions around the metal centers as well as the synergistic effect between S and other doped heteroatoms, the S-C bond and metal sulfides can function as important ORR active sites. Furthermore, the S-doped hybrid sample shows a small charge-transfer resistance. Therefore, S-doping contributes to the superior ORR performance. This chapter describes the recent advancements of S-doped carbon materials, and their development in the area of ORR with regard to components, structures, and their ORR activities of S-related species.

Keywords: S-doping, metal sulfides, sulfur atoms, oxygen reduction reactions, active sites

1. Introduction

Fuel cells are considered as promising energy conversion and storage devices. In such a device, fuels (such as hydrogen, methanol, ethanol, or formic acid) react with oxygen at the anode, while oxygen molecules are reduced to water molecules at the cathode [1–4]. However, the oxygen reduction reaction (ORR) rate is ~5 orders of magnitude slower than the reaction on the anode due to its high overpotential [5]. The search for catalysts that can conquer these huge activation energy barriers has attracted much attention. Although Pt-based electrocatalysts have been commercialized, the high cost of Pt and their poor tolerance to methanol significantly hamper their large-scale commercialization. Thus, great effort has been devoted

IntechOpen

© 2018 The Author(s). Licensee IntechOpen. This chapter is distributed under the terms of the Creative Commons Attribution License (http://creativecommons.org/licenses/by/3.0), which permits unrestricted use, distribution, and reproduction in any medium, provided the original work is properly cited. CC BY

to developing low cost, non-precious-metal, and metal-free catalysts with improved electrocatalytic efficiency [6–9].

Excellent electrocatalysts for ORR should possess a high specific surface area, finely tuned pore structure, and good electron conductivity. The former two facilitate easy accessibility to the active sites and ion diffusion, and the latter is beneficial for electron transfer. Much attention has been focused on the carbonaceous materials due to their remarkable advantages, such as low cost, facile preparation strategy, and high conductivity. For constructing ORR catalysts with promising electrocatalytic activity, single atom doping or co-doping of two or multiple heteroatoms are essential. Metal/nitrogen/carbon (M/N/C) catalysts have been regarded as the most promising alternative for precious metal catalysts. For example, Fe species not only facilitate the formation of catalytically active N-C sites, but Fe atoms also contribute to the graphitization of carbon. More importantly, Fe atoms and related nanoparticles are generally suggested as the active site of ORR catalysts. Recently, the introduction of nonmetal heteroatoms such as N, P, S, or B into carbon materials is generally effective in enhancing ORR activities of catalysts. In N-doped carbon, the N atom with higher electronegativity (3.04) than that of carbon (2.55) leads to more charged adjacent C atoms. With respect to S, the electronegativity of S (2.58) is similar to that of carbon; however, S can easily change the band gap of carbon due to its two lone pair electrons [2]. P with an electronegativity of 2.19 and B with an electronegativity of 2.04 can also induce imbalanced charge distribution in carbon materials, thus forming positively polarized C-P and C-B more active sites to ORR [10, 11]. Furthermore, N/B, N/P, N/S, and N/S/P co-doped carbons also show excellent catalytic activity due to their synergistic effects on spin or charge density of carbon matrix. Notably, designing a carbon matrix with different morphologies combined with hierarchical porous structures, such as micro-, meso-, and macroporosity, can further optimize ORR activity.

Recently, the S atom has attracted particular interest and especially its high synergetic effect with N dopants and metal dopants [12–19]. In this chapter, we briefly summarize the S-related species as active sites in the ORR, such as S-M/N/C, metal chalcogenides, N/S, and N/S/P. We then discuss the S-containing electrocatalysts including their carbon sources, heteroatom dopants, and preparation methods as well as the nanostructure of the supports.

2. S-related active sites in the ORR

The development of novel strategies for the design and synthesis of carbon-based high performance electrocatalysts is a hot topic. Therefore, efforts have been made toward the design and synthesis of extraordinary ORR catalytic carbon materials with different morphologies and single or multiple active sites from diverse sources. S-related active sites have been extensively investigated due to their excellent performance in ORR. S atom mono-doping can induce structural defects in the carbon matrix. The resulting charge dislocation can improve the oxygen adsorption. Furthermore, protonation of S is not as severe as that of N [20]. More importantly, dual doping of N and S or multiple doping of N, S, and M [21] can dramatically enhance ORR activity due to the synergistic effects.

http://dx.doi.org/10.5772/intechopen.78647

2.1. M-N-S-based active sites

Wu et al. prepared Fe, N, and S decorated hierarchical carbon layers (S, N-Fe/N/C-CNT) from pyrolysis of 2,2-bipyridine and $Fe(SCN)_3$-coated CNTs [22]. Adding S salts not only contributed to the formation of atomically dispersed Fe-N_x species, but also improved the surface area of the carbon matrix. The half-wave potential ($E_{1/2}$) of the S,N-Fe/N/C-CNT catalyst is about 0.85 V, which is higher than that of commercial Pt/C (0.82 V). The catalyst also exhibited superior durability in alkaline medium. Theoretical calculations predicted that atomically dispersed Fe-N_x species function as highly active sites, while co-doping of N and S improved the electrical conductivity. Furthermore, Wan et al. fabricated a sandwich-like graphene/carbon hybrid from graphene oxide (GO) and nontoxic starch (**Figure 1**) [23]. Graphene/carbon nanosheets decorated by N, S, and Fe (Fe, S/NGC) were obtained via treatment with $FeCl_3$ and KSCN. Fe,S/NGC showed outstanding ORR performance in alkaline medium ($E_{1/2}$ of 0.83 V vs. RHE, surpassing $E_{1/2}$ of NGC (0.76 V) and the Pt/C catalyst (0.81 V)), due to the simultaneous introduction of Fe and S. The Fe_3N and S were considered major active centers in this hybrid. Furthermore, Fe,S/NGC also displayed a high ORR activity in the acidic solution. In addition, an S and N dual-doped Fe-N-S electrocatalyst (Fe-M-LA/C) was obtained via pyrolysis of the mixture of melamine, lipoic acid, $FeCl_3$, and carbon black [24]. FeS and Fe_3C formed in the Fe-M-LA/C. It has been suggested that Fe^{2+} has high catalytic activity in ORR and that Fe_3C is the active site for the ORR. Combined with the N and S-doping, Fe-M-LA/C showed promising ORR activity. Interestingly, sewage sludge itself can be used as "all-in-one" precursor for ORR catalysts [25]. The innate N, Fe, and S compounds in the sewage sludge function as N, Fe, and S dopants. The N, Fe, and S self-doped nanoporous carbon material exhibited favorable electrocatalytic activity in both alkaline and acidic environments. The nanostructure of the carbon matrix also played an important role in ORR. Wan et al. synthesized Fe/N/S-doped carbon from glucose, thiourea, and iron nitrate based on a dual-template method. Multiple active sites such as graphitic-N, pyridinic-N, thiophene-S, FeN_x,

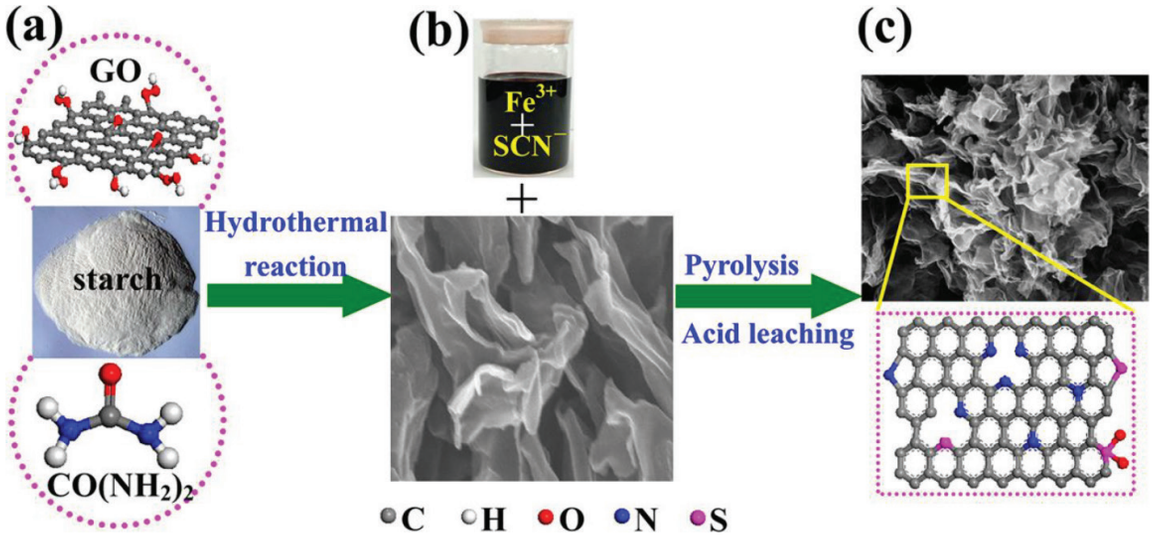

Figure 1. (a) The raw materials of synthesis of NGC nanosheets used as the precursor of Fe,S/NGC-900. (b) Mixed aqueous solution of $FeCl_3$ and KSCN (above) and NGC nanosheets prepared by hydrothermal reaction (below). (c) The as-obtained catalyst (above) and illustration of nitrogen and sulfur atoms in carbon skeleton (below) of Fe,S/NGC-900.

and encapsulated iron nanoparticles combined with hierarchical porous structures contributed to the excellent ORR performance [2].

Bimetal-based N and S doped catalysts have also been reported. Li et al. synthesized PdW alloy nanoparticles decorated S-doped graphene via a microwave irradiation method [26]. S-doping contributed to the formation of small particles and the uniform distribution of alloy particles. The as-prepared catalyst was highly active for ORR due to the specific electronic structure of the alloy. $CoFe_2O_4$ nanoparticles decorated rGO designed by Yang et al. demonstrated high ORR activity due to the existence of defects resulting from the doping of N and S and the covalent coupling between the $CoFe_2O_4$ and rGO matrix [27]. Moreover, Ren et al. synthesized PdNi decorated N and S co-doped three-dimensional ordered carbon derived from acrylonitrile telomere (C, N, and S sources) using silica as template [28]. Due to the co-doping of N and S, the strong electronic interaction between Pd and Ni, and three-dimensional honeycomb-ordered structure, the electrocatalyst exhibited superior performance compared to commercial Pd/C in alkaline solution.

2.2. Metal chalcogenide-based active sites

Wang et al. prepared a raisin bread-like N and S co-doped mesoporous graphitic carbon spheres with $Fe_{1-x}S$ nanocrystals embedded in ($Fe_{1-x}S$/N, S-MGCS) (**Figure 2**) [29]. The $Fe_{1-x}S$/N, S-MGCS catalyst was obtained via pyrolysis of Fe^{2+}-Polydopamine (PDA), followed by a vulcanization process, in which Fe_xC_y was transformed into $Fe_{1-x}S$. This catalyst showed excellent ORR performance in both alkaline medium and acidic medium. Notably, the corresponding E_{onset} and $E_{1/2}$ of $Fe_{1-x}S$/N and S-MGCS were 0.97 and 0.91 V, respectively. The RHE was superior to that of the commercial Pt/C catalyst with an E_{onset} of 0.93 V and an $E_{1/2}$ of 0.87 V. Similarly, Wang et al. prepared a S-Fe/N/C electrocatalyst by pyrolyzing thiourea and iron acetate [30]. Five types of nanoparticles were detected: Fe, FeS, FeN, FeC, and Fe_3O_4. The catalyst showed higher ORR performance compared to Fe/N/C both in alkaline and acidic media. Apparently, more S doping contributed to the higher catalytic performance.

Cobalt chalcogenides as active sites have also attracted significant attention. For example, Li et al. successfully anchored Co_9S_8 nanoparticles on N and S dual doped carbon nanosheets (Co_9S_8/N,S-CNS) via facile pyrolysis of $CoCl_2$, citric acid, and thiourea as carbon source and cubic NaCl crystals were used as template (**Figure 3**) [31]. Due to the highly dispersed nanoparticle and the synergistic catalytic effect between Co_9S_8 nanoparticles and the doped N

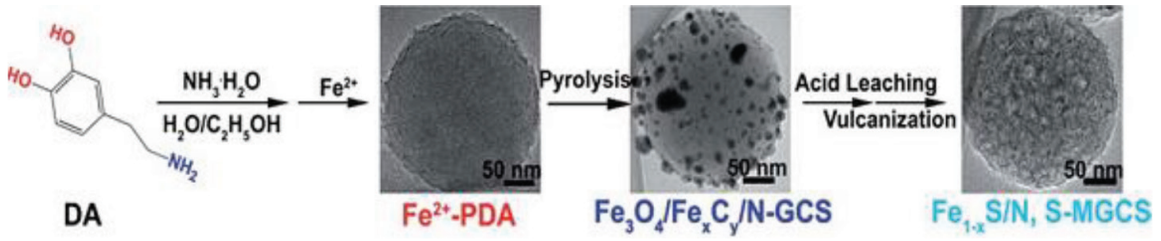

Figure 2. Schematic graph of the formation process from DA to $Fe_{1-x}S$/N, S-MGCS. Reproduced with permission from Ref. [29]. Copyright 2017, Royal Society of Chemistry.

http://dx.doi.org/10.5772/intechopen.78647

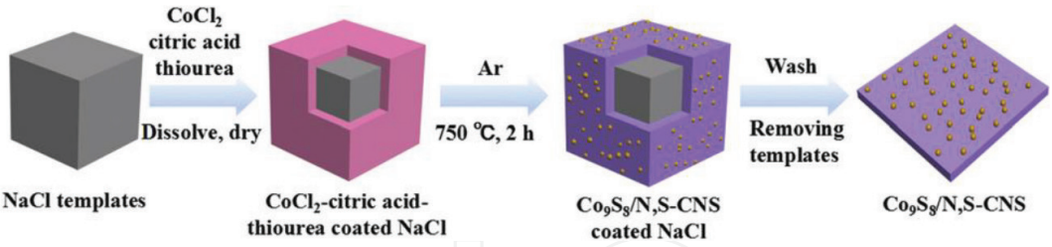

Figure 3. Schematic of the formation of Co_9S_8/N,S-CNS. Reproduced with permission from Ref. [31]. Copyright 2017, Royal Society of Chemistry.

and S in the carbon nanosheets, Co_9S_8/N,S-CNS showed high catalytic activity and stability. Moreover, Liao et al. prepared S co-doped graphene nanoholes with cobalt sulfide hollow nanospheres decorated in ($Co_{1-x}S$/N-S-G) using GO (graphene oxide), phen, and S [32]. The catalyst presented high ORR catalytic activity with an $E_{1/2}$ of 30 mV, which was more positive than that of a commercial Pt/C catalyst. Similarly, Zhang et al. prepared CoS decorated N, S co-doped reduced GO aerogel showing highly efficient activity for ORR [33].

There are other metal sulfides as active sites in ORR. Suh et al. prepared nano-CuS@Cu-BTC composites using Cu-MOF as a sacrificial template and thioacetamide as sulfide source [34]. With the increasing amount of nano-CuS in the composite, electrical conductivity increased, thus contributing to the positive shifts of E_{onset}. MoS_2-embedded nitrogen-doped porous carbon nanosheets were prepared using MoS_2 nanosheets as templates and conjugated microporous polymers as N and C sources [35]. The novel electrocatalysts showed enhanced performance for ORR, due to their strong interaction between MoS_2 and carbon layer, high conductivity, and high specific surface area. Recently, it has been reported that Ni_3S_2 [36] and WS_{3-x} [37] are also potential catalyst for ORR. Furthermore, metallic double sulfides as an ORR catalyst were investigated in recent years. Li et al. prepared $NiCo_2S_4$ and N, S-doped graphene aerogel hybrid for application in ORR [38].

2.3. N-, S-, B-, and P-based active sites

Recently, metal-free catalysts have received much attention, and intensive research efforts have been made. For example, Sun et al. synthesized N,S-co-doped nanocarbon polyhedral morphology using a metal organic framework (MOF) as precursor followed by thermal treatment with ammonia gas (NH_3) and further co-doping of S (**Figure 4**) [39]. The obtained catalyst showed improved electrocatalytic efficiency, comparable to that of the Pt/C catalyst.

Mu et al. synthesized N and S dual-doped 3D porous graphene from waste biomass and GO (**Figure 5**) [40]. The resultant catalyst showed high ORR performance and stability comparable to commercial Pt/C in both alkaline and acidic media due to their unique porous structure and synergistic effects of N and S doping. Furthermore, Wang et al. prepared N and S co-doped 3D hollow structured carbon spheres based on a soft template method [41]. Aniline and pyrrole function as carbon source and N dopant and Na_2S serve as S dopant. The obtained hollow carbon spheres with uniform size, mesoporous structure, and high number of active sites exhibited high ORR activity comparable to that of Pt/C. In contrast, Liao et al.

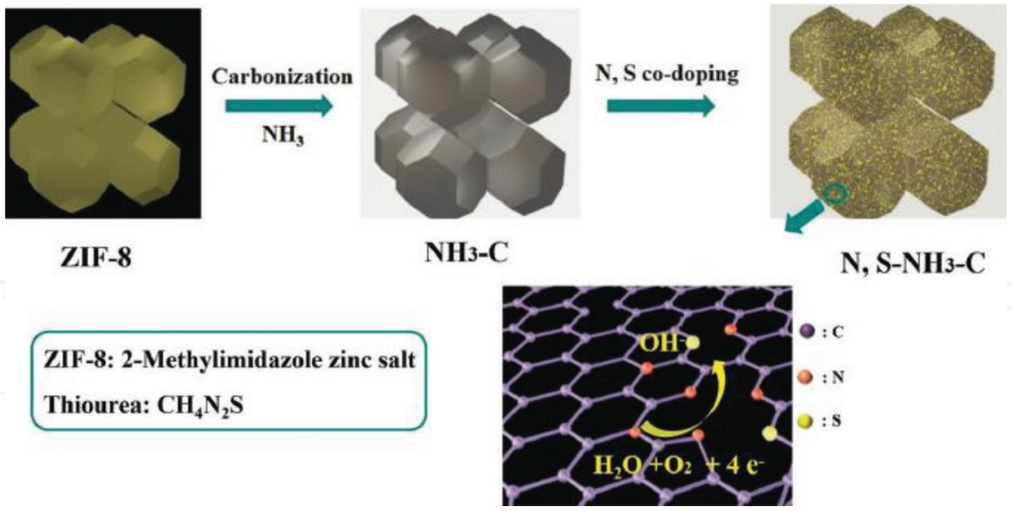

Figure 4. Schematic illustration of the fabrication of the N,S-co-doped nanocarbon as the electrocatalyst toward ORR. The ZIF-8 precursor and thiourea are used as C/N and S precursors, respectively. Reproduced with permission from Ref. [39]. Copyright 2017, Royal Society of Chemistry.

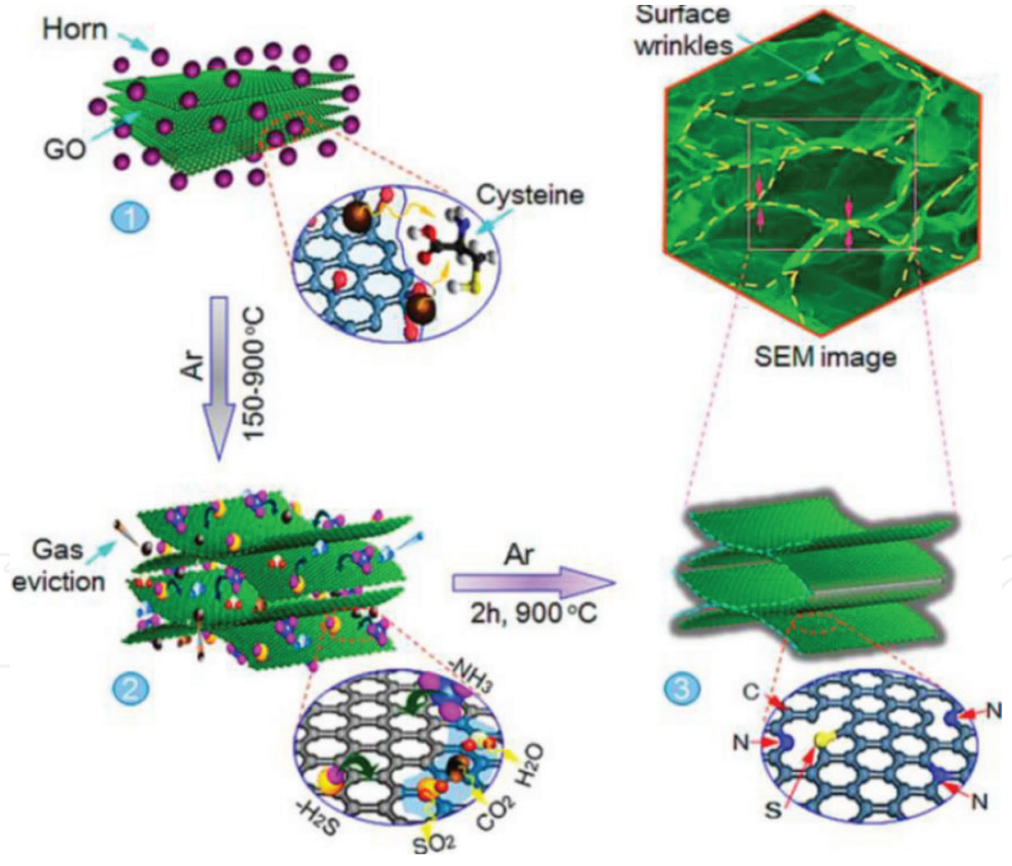

Figure 5. Schematic illustration of the formation of NSG: (stage 1) homogeneous mixture of graphene oxide and horn, (stage 2) disintegration/release of cysteine moieties and coverage of GO surface leading to reaction of functional groups, eviction of gaseous species, and the formation of S and N containing moieties (e.g., H_2S, NH_3, etc.), and (stage 3) doping of N and S into the graphene carbon network. Reproduced with permission from Ref. 40. Copyright 2016, American Chemical Society.

http://dx.doi.org/10.5772/intechopen.78647

prepared N and S co-doped hollow carbon nanospheres from polyacrylonitrile and S via a hard template method [42]. They reported that S-doping facilitated the formation of pyridinic N, which is more active than other N species in ORR. The catalyst exhibits excellent ORR performance with high stability and selectivity.

Dai et al. reported the development of N, S co-doped graphitic sheets from melamine (as carbon precursor and nitrogen dopant), Ni_2SO_4 (as S dopant and template), and KCl (as template) [43]. The unique hierarchical porous structure renders active sites easily accessible and facilitates electron and mass transfer. Therefore, this catalyst was not only effective in ORR, but also demonstrated excellent activities in OER/HER. In addition, Zhi et al. reported that atomic S doping in mesoporous carbon-supported C_3N_4 can remarkably enhance ORR activity [44]. In this work, thiourea was selected as S dopant and C_3N_4 serve as N source. XPS analysis showed the formation of $C_3N_{4-x}S_x$, indicating the atomic modification over the C_3N_4.

Song et al. prepared S-N dual doped ordered mesoporous carbon based on a hard template method [45]. In their work, polythiophene (PTh) and polypyrrole (PPy) were used as precursors and ordered mesoporous silica (SBA-15) was selected as template. Based on this method, N and S contents can be easily adjusted. Furthermore, the mesoscopic morphology provided more accessible active sites. Therefore, this catalyst showed excellent ORR performance.

Recently, P/S binary-doped carbon materials have also been reported. P, with higher electron-donating ability, heavily affects neighboring carbon atoms, thus tending to induce more active sites than N. For instance, Cao et al. prepared P/S co-doped porous carbon derived from resorcinol, furaldehyde, and phosphorus pentasulfide. Due to the synergetic merits of P and S, the onset potential positively shifted for ORR in alkaline media [46].

2.4. Mechanism

In fact, the mechanism of S-related active sites in ORR is still debated. Suib et al. prepared S-doped carbon nanotube-graphene nanolobes via sequential bidoping strategy, in which the nature of S functionalization can be finely tuned [47]. First, thiourea functioned as the S source. To further stabilize and enhance the content of S, the second doping of benzyl disulfide was introduced. Different doping types of S were detected, such as C-S, C-S-C, and -SO_x-. The S-doped CNT showed high catalytic activity and good stability for ORR. Furthermore, Guo et al. studied the effect of Fe/N/C and C-S-C active sites in alkaline and acidic media [48]. It is worth noting that no Fe-S bond formed in the catalyst. They found that no synergistic effects between Fe/N/C and C-S-C were observed in alkaline solution as the two active centers are separated. In contrast, synergistic effects between Fe/N/C and C-S-C sites remarkably enhanced ORR activity in acidic media because the C-S-C active sites facilitated the 4e- ORR pathway.

Furthermore, S can function as platinum nanowire catalyst anchoring sites. Chen et al. studied the influence of S content on the ORR activity of S-doped graphene supported platinum nanowires (PtNW/SGs) [49]. S doping increased the band gap, while the electrical conductivity decreased. PtNW/SGs with 1.40 at% S showed the best ORR performance. Zhi et al.

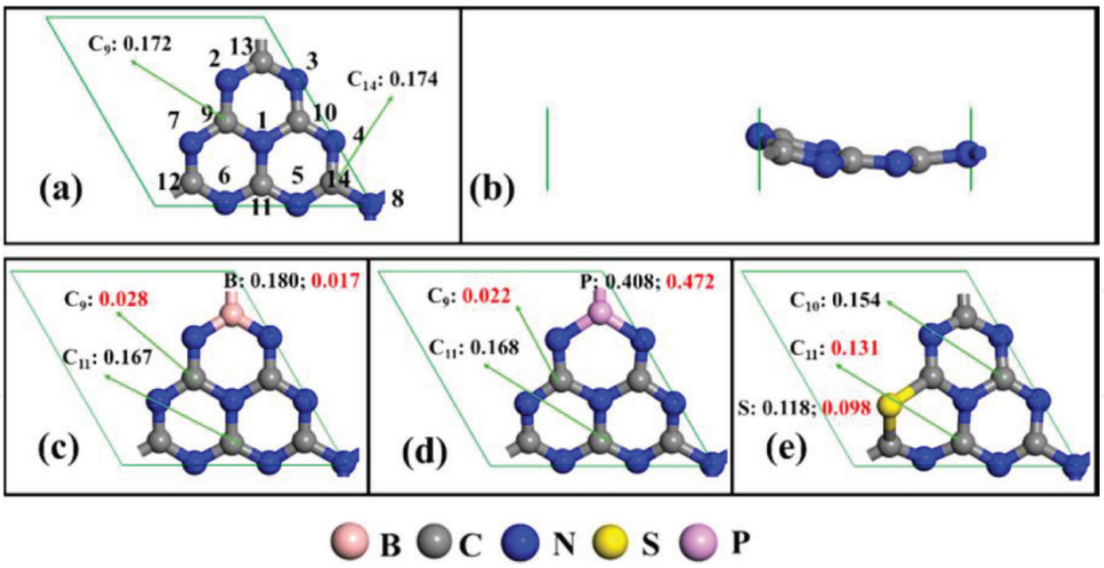

Figure 6. Optimized structure of pristine g-C_3N_4 as (a) top view and (b) side view, in which the N atoms are numbered from 1 to 8, while C atoms are numbered from 9 to 14. Top views of the optimized structures of the energetically most favorable (c) B-CN, (d) P-CN, and (e) SCN, in which the B and P atoms substitute the bay carbon C13, while S atom replaces the pyridinic nitrogen N7. In each structure, the largest value of charge and spin densities on carbon atoms are indicated by black and red colors, respectively; additionally, the related carbon atoms are illustrated by green arrows. Reproduced with permission from Ref. [50]. Copyright 2017, American Chemical Society.

investigated the componential influences of heteroatoms doping (B, P, and S) in graphitic C_3N_4 (g-C_3N_4)-based electrocatalysts (**Figure 6**) [50]. They found that S-doped C_3N_4 with the smallest charge-transfer resistance dramatically boosted the reaction kinetics and activities of ORR.

Recently, Xu et al. designed Fe-N-, Fe-S-, and Fe-N-S-based model catalysts to investigate heteroatom induced performance differences in ORR [51]. Pyrrole-derived and thiophene-derived hypercrosslinked polymers were selected as carbon precursors. $FeCl_3$, a Friedel-Crafts reaction catalyst, acts as both a metal dopant and a porogen. Interestingly, $Fe_{1-x}S$ and Fe_3O_4 nanoparticles formed in the S-doped and N-doped carbon, respectively. In fact, N/Fe_3O_4 acts as a higher catalytic active site than S/$Fe_{1-x}S$. The possible reason is that the strong electronegativity of N generates more charged active sites, while the electronegativity of S is similar to that of carbon. However, the synergistic effect between $Fe_{1-x}S$/Fe_3O_4 and the N, S-doped carbon showed superior ORR performance.

3. Conclusions

Although state-of-the-art Pt-based ORR catalysts are applicable in fuel cell vehicles, source scarcity limits their mass application. M-N-C materials are still far from satisfaction for commercialization. Presently, design and synthesis of novel ORR catalysts with various structures were at the center of research. Furthermore, to experimentally and theoretically explore the relationship between component structure-properties has attracted extensive interest.

http://dx.doi.org/10.5772/intechopen.78647

Particularly, tuning the mode of heteroatom-doping and the underlying the role of active sites in ORR catalysis still remains challenging.

Currently, S-related species represent promising active sites for ORR catalysis. S doping can lead to a higher degree of graphitization because S can react with imperfect carbon to form CS_2 gas [52]. Furthermore, S-doping can modify the spin density distributions around the carbon framework. More importantly, the synergistic effect between the metal center and the N, S-codoped carbon contributes to the superior ORR performance. With regard to metal free catalysts, first-principle calculations indicate that N and S atoms close to each other were more active than isolated N and S sites, indicating a synergistic effect of N and S. Therefore, S-related active sites containing ORR catalyst will be promising alternatives for commercial Pt/C catalysts, especially those with hierarchical porous structures.

Acknowledgements

This work was supported by the National Nature Science Foundation of China (No. 21603156), Jiangsu Province Science Foundation for Youths (No. BK20170331).

Acronyms and abbreviations

ORR	oxygen reduction reaction
PEM	proton exchange membrane
Pt/C	platinum/carbon black catalyst
CB	carbon black
CNT	carbon nanotube
XPS	X-ray photoelectron spectroscopy
$FeCl_3$	iron(III) chloride
KSCN	potassium sulfocyanide
NH_3	ammonia gas
OER	oxygen evolution reaction
HER	hydrogen evolution reaction
rGO	reduced graphene oxide
P	phosphorus
(M/N/C)	metal/nitrogen/carbon

Author details

Dan Xu and Winston Duo Wu*

*Address all correspondence to: duo.wu@suda.edu.cn

Suzhou Key Laboratory of Green Chemical Engineering, School of Chemical and Environmental Engineering, College of Chemistry, Chemical Engineering and Materials Science, Soochow University, Suzhou, China

References

[1] Xia W, Mahmood A, Liang Z, Zou R, Guo S. Earth-abundant nanomaterials for oxygen reduction. Angewandte Chemie, International Edition. 2016;**55**:2650-2676. DOI: 10.1002/anie.201504830

[2] Kone I, Xie A, Tang Y, Chen Y, Liu J, Chen Y, Sun Y, Yang X, Wan P. Hierarchical porous carbon doped with iron/nitrogen/sulfur for efficient oxygen reduction reaction. ACS Applied Materials & Interfaces. 2017;**9**:20963-20973. DOI: 10.1021/acsami.7b02306

[3] Zhang C, An B, Yang L, Wu B, Shi W, Wang YC, Long LS, Wang C, Lin W. Sulfur-doping achieves efficient oxygen reduction in pyrolyzed zeolitic imidazolate frameworks. Journal of Materials Chemistry A. 2016;**4**:4457-4463. DOI: 10.1039/c6ta00768f

[4] Zhu J, Li K, Xiao M, Liu C, Wu Z, Ge J, Xing W. Significantly enhanced oxygen reduction reaction performance of N-doped carbon by heterogeneous sulfur incorporation: Synergistic effect between the two dopants in metal-free catalysts. Journal of Materials Chemistry A. 2016;**4**:7422-7429. DOI: 10.1039/c6ta02419j

[5] Sui S, Wang X, Zhou X, Su Y, Riffat S, Liu CJ. A comprehensive review of Pt electrocatalysts for oxygen reduction reaction: Nanostructure, activity, mechanism and carbon support in PEM fuel cells. Journal of Materials Chemistry A. 2017;**5**:1808-1825. DOI: 10.1039/c6ta08580f

[6] Jin X, Xie Y, Huang J. Highly effective dual transition metal macrocycle based electrocatalyst with macro−/mesoporous structures for oxygen reduction reaction. Catalysts. 2017;**7**:201. DOI: 10.3390/catal7070201

[7] Akhter T, Islam MM, Faisal SN, Haque E, Minett AI, Liu HK, Konstantino K, Dou SX. Self-assembled N/S codoped flexible graphene paper for high performance energy storage and oxygen reduction reaction. ACS Applied Materials & Interfaces. 2016;**8**:2078-2087. DOI: 10.1021/acsami.5b10545

[8] Oh S, Kim JH, Kim M, Nam D, Park JY, Cho EA, Kwon HS. Synergetic effects of edge formation and sulfur doping on the catalytic activity of a graphene-based catalyst for the oxygen reduction reaction. Journal of Materials Chemistry A. 2016;**4**:14400-14407. DOI: 10.1039/c6ta05020d

[9] Bhange SN, Unni SM, Kurungot S. Nitrogen and sulphur co-doped crumbled graphene for the oxygen reduction reaction with improved activity and stability in acidic medium. Journal of Materials Chemistry A. 2016;**4**:6014-6020. DOI: 10.1039/c6ta00073h

[10] Razmjooei F, Singh KP, Yu JS. Superior pore network retention of carbon derived from naturally dried ginkgo leaves and its enhanced oxygen reduction performance. Catalysis Today. 2016;**260**:148-157. DOI: 10.1016/j.cattod.2015.06.012

[11] Tong Y, Chen P, Zhou T, Xu K, Chu W, Wu C, Xie Y. A bifunctional hybrid electrocatalyst for oxygen reduction and evolution: Cobalt oxide nanoparticles strongly coupled to B,N-decorated graphene. Angewandte Chemie, International Edition. 2017;**56**:1-6. DOI: 10.1002/anie.201702430

[12] Wu M, Liu Y, Zhu Y, Lin J, Liu J, Hu H, Wang Y, Zhao Q, Lv R, Qiu J. Supramolecular polymerization-assisted synthesis of nitrogen and sulfur dual-doped porous grapheme networks from petroleum coke as efficient metal-free electrocatalysts for the oxygen reduction reaction. Journal of Materials Chemistry A. 2017;**5**:11331-11339. DOI: 10.1039/c7ta03264a

[13] Li J, Zhang Y, Zhang X, Huang J, Han J, Zhang Z, Han X, Xu P, Song B. S, N dual-doped graphene-like carbon nanosheets as efficient oxygen reduction reaction electrocatalysts. ACS Applied Materials & Interfaces. 2017;**9**:398-405. DOI: 10.1021/acsami.6b12547

[14] Zhao H, Zhu YP, Ge L, Yuan ZY. Nitrogen and sulfur co-doped mesoporous hollow carbon microspheres for highly efficient oxygen reduction electrocatalysts. International Journal of Hydrogen Energy. 2017;**42**:19010-19018. DOI: 10.1016/j.ijhydene.2017.06.172

[15] Yao Y, You Y, Zhang G, Liu J, Sun H, Zou Z, Sun S. Highly functional bioinspired Fe/N/C oxygen reduction reaction catalysts: Structure-regulating oxygen sorption. ACS Applied Materials & Interfaces. 2016;**8**:6464-6471. DOI: 10.1021/acsami.5b11870

[16] Huo L, Liu B, Zhang G, Si R, Liu J, Zhang J. 2D layered non-precious metal mesoporous electrocatalysts for enhanced oxygen reduction reaction. Journal of Materials Chemistry A. 2017;**5**:4868-4878. DOI: 10.1039/c6ta10261a

[17] Liu T, Guo YF, Yan YM, Wang F, Deng C, Rooney D, Sun KN. CoO nanoparticles embedded in three-dimensional nitrogen/sulfur co-doped carbon nanofiber networks as a bifunctional catalyst for oxygen reduction/evolution reactions. Carbon. 2016;**106**:84-92. DOI: 10.1016/j.carbon.2016.05.007

[18] Mulyadi A, Zhang Z, Dutzer M, Liu W, Deng Y. Facile approach for synthesis of doped carbon electrocatalyst from cellulose nanofibrils toward high-performance metal-free oxygen reduction and hydrogen evolution. Nano Energy. 2017;**32**:336-346. DOI: 10.1016/j.nanoen.2016.12.057

[19] Su Y, Yao Z, Zhang F, Wang H, Mics Z, Cánovas E, Bonn M, Zhuang X, Feng X. Sulfur-enriched conjugated polymer nanosheet derived sulfur and nitrogen co-doped porous carbon nanosheets as electrocatalysts for oxygen reduction reaction and zinc-air battery. Advanced Functional Materials. 2016;**26**:5893-5902. DOI: 10.1002/adfm.201602158

[20] Zhang L, Wang Y, Wan K, Piao JH, Liang ZX. Effective sulfur-doping in carbon by high-temperature molten salt bath and its electrocatalysis for oxygen reduction reaction. Electrochemistry Communications. 2018;**86**:53-56. DOI: https://doi.org/10.1016/j.elecom.2017.11.015

[21] Zhu YN, Cao CY, Jiang WJ, Yang SL, Hu JS, Song WG, Wan LJ. Nitrogen, phosphorus and sulfur co-doped ultrathin carbon nanosheets as a metal-free catalyst for selective oxidation of aromatic alkanes and the oxygen reduction reaction. Journal of Materials Chemistry A. 2016;**4**:18470-18477. DOI: 10.1039/c6ta08335h

[22] Chen P, Zhou T, Xing L, Xu TY, Xie H, Zhang L, Yan W, Chu W, Wu C, Xie Y. Atomically dispersed iron–nitrogen species as electrocatalysts for bifunctional oxygen evolution and reduction reactions. Angewandte Chemie, International Edition. 2017;**56**:610-614. DOI: 10.1002/anie.201610119

[23] Men B, Sun Y, Liu J, Tang Y, Chen Y, Wan P, Pan J. Synergistically enhanced electrocatalytic activity of sandwich-like N-doped graphene/carbon nanosheets decorated by Fe and S for oxygen reduction reaction. ACS Applied Materials & Interfaces. 2016;**8**:19533-19541. DOI: 10.1021/acsami.6b06329

[24] Huang HC, Lin YC, Chang ST, Liu CC, Wang KC, Jhong HP, Lee JF, Wang CH. Effect of a sulfur and nitrogen dual-doped Fe-N-S electrocatalyst for the oxygen reduction reaction. Journal of Materials Chemistry A. 2017;**5**:19790-19799. DOI: 10.1039/c7ta05030e

[25] Yuan SJ, Dai XH. Facile synthesis of sewage sludge derived in-situ multi-doped nanoporous carbon material for electrocatalytic oxygen reduction. Scientific Reports. 2016;**6**:27570. DOI: 10.1038/srep27570

[26] Li Y, Li W, Ke T, Zhang P, Ren X, Deng L. Microwave-assisted synthesis of sulfur-doped graphene supported PdW nanoparticles as a high performance electrocatalyst for the oxygen reduction reaction. Electrochemistry Communications. 2016;**69**:68-71. DOI: 10.1016/j.elecom.2016.06.006

[27] Yan W, Cao X, Tian J, Jin C, Ke K, Yang R. Nitrogen/sulfur dual-doped 3D reduced graphene oxide networkssupported $CoFe_2O_4$ with enhanced electrocatalytic activities for oxygen reduction and evolution reactions. Carbon. 2016;**99**:195-202. DOI: 10.1016/j.carbon.2015.12.011

[28] Li Y, Lin S, Ren X, Mi H, Zhang P, Sun L, Deng L, Gao Y. One-step rapid in-situ synthesis of nitrogen and sulfur co-doped three-dimensional honeycomb-ordered carbon supported PdNi nanoparticles as efficient electrocatalyst for oxygen reduction reaction in alkaline solution. Electrochimica Acta. 2017;**253**:445-454. DOI: 10.1016/j.electacta.2017.08.143

[29] Xiao JW, Xia YT, Hu CC, Xi JGB, Wang S. Raisin bread-like iron sulfides/nitrogen and sulfur dual-doped mesoporous graphitic carbon spheres: A promising electrocatalyst for the oxygen reduction reaction in alkaline and acidic media. Journal of Materials Chemistry A. 2017;**5**:11114-11123. DOI: 10.1039/c7ta02096a

[30] Hu K, Tao L, Liu DD, Huo J, Wang SY. Sulfur-doped Fe/N/C Nanosheets as highly efficient electrocatalysts for oxygen reduction reaction. ACS Applied Materials & Interfaces. 2016;**8**:19379-19385. DOI: 10.1021/acsami.6b02078

[31] Wu C, Zhang Y, Dong D, Xie H, Li J. Co_9S_8 nanoparticles anchored on nitrogen and sulfur dual-doped carbon nanosheets as highly efficient bifunctional electrocatalyst for oxygen evolution and reduction reactions. Nanoscale. 2017;**9**:12432-12440. DOI: 10.1039/c7nr03950f

[32] Qiao X, Jin J, Fan H, Li Y, Liao S. In situ growth of cobalt sulfide hollow nanospheres embedded in nitrogen and sulfur co-doped graphene nanoholes as a highly active electrocatalyst for oxygen reduction and evolution. Journal of Materials Chemistry A. 2017;**5**:12354-12360. DOI: 10.1039/c7ta00993c

[33] Luo Z, Tan C, Zhang X, Chen J, Cao X, Li B, Zong Y, Huang L, Huang X, Wang L, Huang W, Zhang H. Preparation of cobalt sulfide nanoparticle-decorated nitrogen and sulfur co-doped reduced graphene oxide aerogel used as a highly efficient electrocatalyst for oxygen reduction reaction. Small. 2016;**12**:5920-5926. DOI: 10.1002/smll.201602615

[34] Cho K, Han SH, Suh MP. Copper–organic framework fabricated with CuS nanoparticles: Synthesis, electrical conductivity, and electrocatalytic activities for oxygen reduction reaction. Angewandte Chemie, International Edition. 2016;**55**:15301-15305. DOI: 10.1002/anie.201607271

[35] Yuan K, Zhuang X, Fu H, Brunklaus G, Forster M, Chen Y, Feng X, Scherf U. Two-dimensional core-shelled porous hybrids as highly efficient catalysts for the oxygen reduction reaction. Angewandte Chemie, International Edition. 2016;**55**:6858-6863. DOI: 10.1002/anie.201600850

[36] Yan B, Concannon NM, Milshtein JD, Brushett FR, Surendranath Y. A membrane-free neutral pH formate fuel cell enabled by a selective nickel sulfide oxygen reduction catalyst. Angewandte Chemie, International Edition. 2017;**56**:1-5. DOI: 10.1002/anie.201702578

[37] Tan SM, Pumera M. Electrosynthesis of bifunctional WS_{3-x}/reduced graphene oxide hybrid for hydrogen evolution reaction and oxygen reduction reaction electrocatalysis. Chemistry—A European Journal. 2017;**23**:1-11. DOI: 10.1002/chem.201701722

[38] Yang T, Li R, Li Z, Gu Z, Wang G, Liu J. Hybrid of $NiCo_2S_4$ and nitrogen and sulphur-functionalized multiple graphene aerogel for application in supercapacitors and oxygen reduction with significant electrochemical synergy. Electrochimica Acta. 2016;**211**:59-70. DOI: 10.1016/j.electacta.2016.06.028

[39] Song Z, Liu W, Cheng N, Banis MN, Li X, Sun Q, Xiao B, Liu Y, Lushington A, Li R, Liu L, Sun X. Origin of the high oxygen reduction reaction of nitrogen and sulfur co-doped MOF-derived nanocarbon electrocatalysts. Materials Horizons. 2017;**4**:900-907. DOI: 10.1039/c7mh00244k

[40] Amiinu IS, Zhang J, Kou Z, Liu X, Asare OK, Zhou H, Cheng K, Zhang H, Mai L, Pan M, Mu S. Self-organized 3D porous graphene dual-doped with biomass-sponsored nitrogen and sulfur for oxygen reduction and evolution. ACS Applied Materials & Interfaces. 2016;**8**:29408-29418. DOI: 10.1021/acsami.6b08719

[41] Wu Z, Liu R, Wang J, Zhu J, Xiao W, Xuan C, Lei W, Wang D. Nitrogen and sulfur co-doping of 3D hollowstructured carbon spheres as an efficient and stable metal free

catalyst for the oxygen reduction reaction. Nanoscale. 2016;**8**:19086-19092. DOI: 10.1039/c6nr06817k

[42] You C, Jiang X, Han L, Wang X, Lin Q, Hua Y, Wang C, Liu X, Liao S. Uniform nitrogen and sulphur co-doped hollow carbon nanospheres as efficient metal-free electrocatalysts for oxygen reduction. Journal of Materials Chemistry A. 2017;**5**:1742-1748. DOI: 10.1039/c6ta08674h

[43] Hu C, Dai L. Multifunctional carbon-based metal-free electrocatalysts for simultaneous oxygen reduction, oxygen evolution, and hydrogen evolution. Advanced Materials. 2017;**29**:1604942. DOI: 10.1002/adma.201604942

[44] Pei Z, Zhao J, Huang Y, Huang Y, Zhu M, Wang Z, Chen Z, Zhi C. Toward enhanced activity of a graphitic carbon nitride-based electrocatalyst in oxygen reduction and hydrogen evolution reactions via atomic sulfur doping. Journal of Materials Chemistry A. 2016;**4**:12205-12211. DOI: 10.1039/c6ta03588d

[45] Jiang T, Wang Y, Wang K, Liang Y, Wu D, Tsiakaras P, Song S. A novel sulfur-nitrogen dual doped ordered mesoporous carbon electrocatalyst for efficient oxygen reduction reaction. Applied Catalysis B: Environmental. 2016;**189**:1-11. DOI: 10.1016/j.apcatb.2016.02.009

[46] Zhou Y, Ma R, Candelaria SL, Wang J, Liu Q, Uchaker E, Li P, Chen Y, Cao G. Phosphorus/sulfur Co-doped porous carbon with enhanced specific capacitance for supercapacitor and improved catalytic activity for oxygen reduction reaction. Journal of Power Sources. 2016;**314**:39-48. DOI: 10.1016/j.jpowsour.2016.03.009

[47] El-Sawy AM, Mosa IM, Su D, Guild CJ, Khalid S, Joesten R, Rusling JF, Suib SL. Controlling the active sites of sulfur-doped carbon nanotube–graphene nanolobes for highly efficient oxygen evolution and reduction catalysis. Advanced Energy Materials. 2016;**6**:1501966. DOI: 10.1002/aenm.201501966

[48] Shen H, Gracia-Espino E, Ma J, Zang K, Luo J, Wang L, Gao S, Mamat X, Hu G, Wagberg T, Guo S. Synergistic effects between atomically dispersed Fe-N-C and C-S-C for the oxygen reduction reaction in acidic media. Angewandte Chemie, International Edition. 2017;**56**:13800-13804. DOI: 10.1002/anie.201706602

[49] Hoque MA, Hassan FM, Seo MH, Choi JY, Pritzker M, Knights S, Ye S, Chen Z. Optimization of sulfur-doped graphene as an emerging platinum nanowires support for oxygen reduction reaction. Nano Energy. 2016;**19**:27-38. DOI: 10.1016/j.nanoen.2015.11.004

[50] Pei ZX, Gu JX, Wang YK, Tang ZJ, Liu ZX, Huang Y, Huang Y, Zhao JX, Chen ZF, Zhi CY. Component matters: Paving the roadmap toward enhanced electrocatalytic performance of graphitic C_3N_4-based catalysts via atomic tuning. ACS Nano. 2017;**11**:6004-6014. DOI: 10.1021/acsnano.7b01908

[51] Zhang J, Xu D, Wang C, Guo J, Yan F. Rational design of $Fe_{1-x}S/Fe_3O_4$/nitrogen and sulfur-doped porous carbon with enhanced oxygen reduction reaction catalytic activity. Advanced Materials Interfaces. 2018:1701641. DOI: 10.1002/admi.201701641

[52] Shih PT, Dong RX, Shen SY, Vittal R, Lin JJ, Ho KC. Transparent graphene–platinum nanohybrid films for counter electrodes in high efficiency dye-sensitized solar cells. Journal of Materials Chemistry A. 2014;**2**:8742-8748. DOI: 10.1039/c3ta12931d

IntechOpen

IntechOpen

IntechOpen

IntechOpen